TECHNICAL MEMORANDUMS

NATIONAL ADVISORY COMMITTEE FOR AERONAUTICS

No. 380

EXPERIMENTS ON AUTOROTATION

By E. Anderlik

From "Zeitschrift für Flugtechnik und Motorluftschiffahrt"
August 28, 1926

Washington
September, 1926

NATIONAL ADVISORY COMMITTEE FOR AERONAUTICS.

TECHNICAL MEMORANDUM No. 380.

EXPERIMENTS ON AUTOROTATION.*

By E. Anderlik.

In recent years many experiments have been tried with models, especially in England, for the purpose of learning something concerning the behavior of an airplane in a spin. This article deals principally with Professor Bairstow's experiments on autorotation, in which the wing is free to rotate about an axis in its plane of symmetry, which axis is parallel with the direction of the wind. An article on experiments of this nature was published in "Zeitschrift für Flugtechnik und Motorluftschiffahrt" 1921, p. 273. Subsequently, several English articles have appeared describing such experiments with various airplane models.

It is already known that the conditions in autorotation and spinning are in so far related that both kinds of motion occur at large mean angles of attack and that one wing tip is in the high angle-of-attack region and the other in the low. Hence the hope of being able to master the aerodynamic part of spinning through autorotation experiments. Recently repeated accidents happened to the English airplane "Bantam," because it was not able to come out of a spin. Therefore the "Accidents Investigation Subcommittee" instituted a systematic investigation, in

* From "Zeitschrift für Flugtechnik und Motorluftschiffahrt," August 28, 1926, pp. 338-342.

which the results obtained by autorotation differed plainly for the "Bantam" from those obtained with other standard airplanes (Aeronautical Research Committee Reports and Memoranda No. 976).

We can obtain no exhaustive information through autorotation experiments, as to what air forces are exerted on a rotating wing. If we wish to utilize the autorotation experiments for determining the conditions in a spin, we must extend these experiments to the point of actually measuring the air forces. As a small step in this direction, we arranged a program of experiments which we will proceed to describe. It was proposed:

1. To make a systematic comparison of various wings in autorotation, in connection with which the effect of the index value will also be studied;

2. To investigate the effect of a side wind on autorotation;

3. To investigate the resistance or drag of a rotating wing.

In this connection, an important question is to be taken up, which originated with Professor Bairstow, namely, the measurement of the pressure distribution on a rotating wing, preparations for which are now being made in England.

For the execution of the above experiments, Professor Bairstow kindly placed at my disposal the wind tunnel of the Imperial College of Science, and Mr. F. F. Crocombe assisted me in the experiments.

Before discussing the experimental results individually, I will briefly describe the conditions in the autorotation. We assumed in advance that the wing, which was free to turn about its axis, would receive a rotary impulse. If we designate the angular velocity by ω, the wind velocity by V, the distance of a wing section from the axis of rotation by y, the wing chord by t and the half span by s, then the change in the angle of attack of the wing section is $\Delta\,\alpha \sim \frac{\omega y}{V}$. There is thus exerted on the wing the moment M about the axis of rotation.

$$M = \rho\, t \int_{-s}^{+s} (c_a \cos\mu + c_w \sin\mu)\,(v^2 + (\omega\, y)^2\,)\, y\, d\, y,$$

in which

$$\mu = \text{arc tan} \frac{\omega\, y}{V}$$

As customary in stability problems, ω is assumed to be small and consequently

$$\cos\mu = 1 - \left(\frac{\omega\, y}{V}\right)^2, \quad c_a\,(\alpha + \Delta\,\alpha) = c_a + \frac{\omega\, y}{V}\,\frac{d\, c_a}{d\,\alpha}\,, \text{ hence}$$

$$M = \rho\, V^2\, t\, \omega\, A\, \frac{d\, C_a}{d\,\alpha} + C_w\,,$$

in which A is a constant, dependent on the distribution of the air forces. (It is assumed that the air forces are uniformly distributed over the wing.) According to this expression, autorotation is to be expected in the angle-of-attack region where

$$\frac{d\, c_a}{d\,\alpha} + c_w < 0.$$

This result had been already obtained by Glauert in a somewhat different manner (A.R.C. Reports and Memoranda No. 595).

For the further processes, this expression simply indicates that, on the half-wing which is functioning with the greater angle of attack, smaller forces act, than on the half-wing which is functioning with the smaller angle of attack, thereby producing a moment which increases ω. Through this increased ω the differences in the angles of attack at the wing tips constantly increase and thus one wing tip comes into such a small angle-of-attack region as to produce at the wing tips a moment which opposes the rotation and continues to increase until the accelerating and damping portions of the moment offset one another and produce uniform rotation. This process was pursued experimentally. Fig. 1 shows two moment curves from the above-mentioned British article. On the upper curve, the moment reaches a maximum and then returns to zero. On the lower curve, there is a back and forth oscillation of the moment before zero is reached. For performing the experiments, we adopted a common form of apparatus to which we will recur. We had at our disposal a wind tunnel with a cross section of 1.22 × 1.52 m (4 × 5 ft.) and a maximum velocity of 21 m (69 ft.) per second. The span of the wing used was about 61 cm (24 inches). The maximum attainable index value, therefore, was E = 12,800 mm m/s.

A series of four airfoils, two thin ones and two thick ones (Fig. 2), was chosen for the experiments. We first measured the lift and drag coefficients and then the autorotational velocities, the latter with a stop watch. The experimental results were so represented that the nondimensional quantity $\frac{\omega s}{V}$ was plotted against the angle of attack and then against the velocity. $\frac{\omega s}{V}$ is approximately the change in the angle of attack between the middle and tip of the wing.

The two thin airfoils (Nos. 1-2) showed nothing new, but the thick airfoils (Nos. 3-4) proved to be well adapted for testing the condition $\frac{d\ c_a}{d\ \alpha} + c_w < 0$. The lift curve shows, in the low index value region, a strong dependence on the index value. Since we can expect autorotation in the region where $\frac{d\ c_a}{d\ \alpha} < 0$, two separate angle-of-attack regions, in which rotation is possible, come into consideration in the case where c_a has two maxima.

As shown in Fig. 3, the lift curve of airfoil No. 3 reaches its maximum at $\alpha = 14.5^\circ$, 15° and 22.5°, corresponding respectively to the wind velocities of 9.15 m (30 ft.), 13.7 m (45 ft.), and 18.3 m (60 ft.) per second. The lift curve at $V = 13.7$ m (45 ft.) per second shows a second maximum at $\alpha = 25^\circ$. The connection between $\frac{d\ c_a}{d\ \alpha} + c_w$ and the autorotation curve (Fig. 4) is perfectly clear. At $\alpha = 19\text{-}20^\circ$ the airfoil does not rotate. Below 20° a rotation was observed for wind velocities not exceeding 15.25 m (50 ft.) per second, but the airfoil did not rotate for $V = 18.3$ m (60 ft.) per second, while rotation occurred in the angle-of-attack region $> 20^\circ$ only for wind velocities of not less than 12.2 m (40 ft.) per second. This is also shown by Fig. 5, in which $\frac{\omega s}{V}$ is plotted against V.

For airfoil No. 4 the conditions are similar, autorotation beginning at $\alpha = 5^\circ$, corresponding to the maximum and to the sudden drop in the lift curve. Since the lift curves (Fig. 6) for the velocities 9.15-21.3 m (30-70 ft.) per second attain their first maximum in the region of $\alpha = 5\text{-}10^\circ$, autorotation is possible in this region for all these velocities. On the other hand there is a second autorotation region present for $\alpha \sim 35^\circ$. Autorotation is observable here, however, only when V exceeds 15.25 m (50 ft.) per second. This indicates that the condition $\frac{d\,c_a}{d\,\alpha} < 0$ does not alone suffice, since c_a attains a maximum for $V = 15.25$ m (50 ft.) per second at $\alpha = 35^\circ$, but $\left(\frac{d\,c_a}{d\,\alpha}\right)_{max} = -0.25$ and in this region $c_w > 0.25$, so that $\frac{d\,c_a}{d\,\alpha} + c_w > 0$ and consequently there is no autorotation. In Relf and Lavender's first article on autorotation (A.R.C. Reports and Memoranda No. 549) ω is given as a function of the velocity V and the connection is indicated by a straight line. If $\frac{\omega s}{V}$ is plotted against V, it follows that $\frac{\omega s}{V}$ is independent of v and hence of the index value. According to what has thus far been said, this result must be recognized as true only for thin airfoils. For thick airfoils, however, a strong dependence on the index value is noticeable (up to index values of -12000 mm m/s). When, therefore, autorotation experiments are to be evaluated for thick wings, it must be endeavored to obtain the highest possible index value in the experiments.

A second series of experiments was performed for the purpose of determining the effect of a lateral wind on autorotation. Similar experiments were tried with the "Bantam." The model was rotated 30° laterally about the axis of rotation, which was parallel to the wind direction. This entirely stopped the autorotation. We tested two airfoils (Nos. 1 and 3) at 5, 10, 15, and 20° lateral angle for wind velocities of 30, 45 and 60 ft. per second. As typical results, two sets of curves for several experiments are given.

In Fig. 8, $\frac{\omega s}{V}$ is again plotted against the angle of attack, each lateral angle having its own $\frac{\omega s}{V}$ curve. Furthermore, (Fig. 9) $\frac{\omega s}{V}$ was plotted against the lateral angle for a given angle of attack ($\alpha = 30°$). The three curves in Fig. 9 are for the three velocities. The airfoil was fastened to a small circular plate (Fig. 10, o) which could be inclined to the axis in various ways. The airfoil was fastened to the plate by a screw (s), which passed through the plate and the center of the airfoil, so that the airfoil could be fastened to the plate in an oblique position corresponding to a given lateral angle.

Figs. 8-9 show that the oblique position of the airfoil produces two effects. First, it increases the $\frac{\omega s}{V}$ values and, second, it considerably extends the upper limit of the autorotation field. These results can stand with the British ones, since a maximum value of $\frac{\omega s}{V}$ seems to exist for $\tau = 20°$ lateral angle. Unfortunately the arrangement did not allow larger lateral angles. In our opinion, the objection may be made to these experiments that the point, around which the wing was turned laterally, did not coincide, in the original position, with the axis of rotation. In this manner an additional moment was produced, so that the above-mentioned results may differ for different positions of the center of rotation. It would be useful to perform these experiments in such a way that the axis of rotation would be turned toward the wind direction, thus subjecting the mean angle of attack to periodical changes. In this case, the rotational velocity of the airfoil would have to be obtained with a recording instrument, in order to determine the rotational accelerations.

Our third series of experiments was carried out for the purpose of determining the drag of the rotating airfoil. The rear end of the axis, about which the airfoil rotated, was articulated with an aerodynamic balance (Fig. 11) and the forward portion was suspended on two wires. The rear end of the axis was secured laterally by wires, in order to protect the balance from lateral stresses (perpendicular to V). This arrangement afforded perfect freedom of motion in the wind direction. In performing the experiments, readings were made on the balance for both rotating and stationary airfoils. The difference between these readings equals the difference in the drag between the rotating and stationary airfoils. Of course the revolution number of the airfoil was also taken. The experimental results are so presented as to include the drags (c_{wr}) in the drag curves of the rotating airfoil.

This drag can be calculated on the basis of simplifying assumptions, if we assume as heretofore, that the change in the angle of attack $\left(\frac{\omega\, y}{V}\right)$ varies directly as y and that the air stresses are uniformly distributed, and if the radial velocity is disregarded. With the earlier designations, the drag is

$$W_R = \rho\, V^2\; t \int_{-s}^{+s} (c_w \cos\mu - c_a \sin\mu) \quad 1 + \left(\frac{\omega\; y}{V}\right)^2 \; d\; y$$

or, if $\frac{\omega\, y}{V} = \zeta$ is introduced and the third and fourth powers of ζ are disregarded.

$$W_R = \frac{\rho\; V\; t}{\omega} \left[\int_{\frac{\omega s}{V}}^{+\frac{\omega s}{V}} c_w\, d\,\zeta - \int_{-\frac{\omega s}{V}}^{+\frac{\omega s}{V}} c_a\, \zeta\; d\; \zeta \right]$$

or. if the coefficient of drag is to be calculated,

$$c_{wr} = \frac{V}{\omega\;\, s}\,(f - m).$$

in which f and m serve as abbreviations for the earlier integrals. The values of f and m can be indicated simply and determined with corresponding ease. If a portion of the surface in the lift and drag curves is limited by the straight lines $\alpha \pm \frac{\omega\; s}{V}$, then f is the area of this portion in the c_w curve and m is the moment of the surface portion in the c_a curve with respect to the line α. Hence f and m must be graphically determined in such a manner that an integral curve will be constructed for c_w curve and a rope polygon for the c_a curve. We know that, with the results obtained by this computation, the essential thing is not yet mastered. The computed c_{wr} values serve simply as a basis of comparison for showing the deviations from these assumptions.

Both the measured and the computed drag coefficients of the rotating airfoil are introduced into the drag curves for airfoils 1 and 3. For these airfoils, the measurements were made at three speeds. As shown in Fig. 12, the differences $c_w - c_{wr}$ are positive throughout for airfoil No. 1, showing that the drag is somewhat decreased by the rotation. The order of magnitude of this difference is 0.02 - 0.04, corresponding to a deviation of 10%. It is surprising that the computed c_{wr} values agree well with the observed. Even if such agreement can not be demonstrated on other thin airfoils, the moment which operates in the airfoil plane can be computed with the help of the autorotation curve, so that we would obtain the expression

$$N = \frac{V^4}{\omega^2} \varphi (\alpha)$$

in which $\varphi (\alpha)$ is a (definite) function of the angle of attack.

The conditions are different for the thick airfoil No. 3.

The differences $c_w - c_{wr}$ are plus and minus and their order of magnitude is 0.1, which means 30-40% in the ratio of the c_w values. Here the computed drag coefficients do not agree at all with the measured ones, as shown by Figs. 13-15. The computation could not be made in connection with the drag measurement for the maximum velocity, since the drag and lift measurements were not extended to sufficiently large angles of attack.

A more accurate investigation of autorotation, in the present status of our knowledge of flow phenomena, seems to be very difficult. Hence even the results given here are not at all conclusive, but we hope that further experiments of this kind will make valuable contributions to our knowledge of the conditions of motion in a spin.

Translation by Dwight M. Miner,
National Advisory Committee
for Aeronautics.

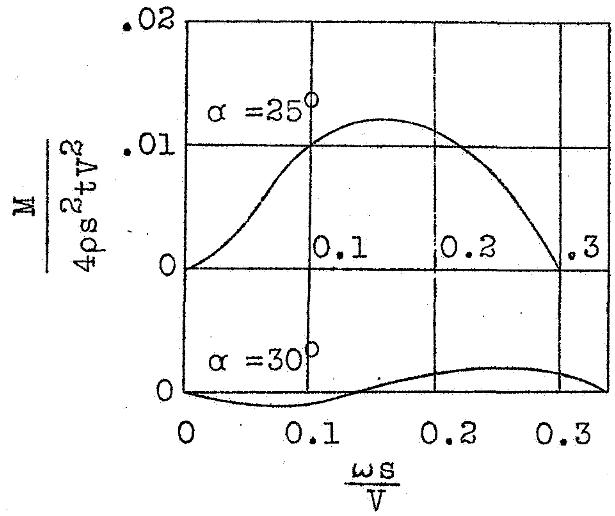
.02
α =25°
.01
0
0.1
0.2
.3
α =30°
0
0
0.1
0.2
0.3
$\frac{M}{4\rho s^2 t V^2}$
$\frac{\omega s}{V}$

Fig.1

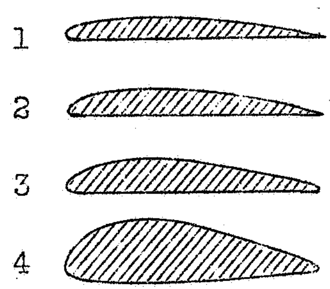
1
2
3
4

Fig.2

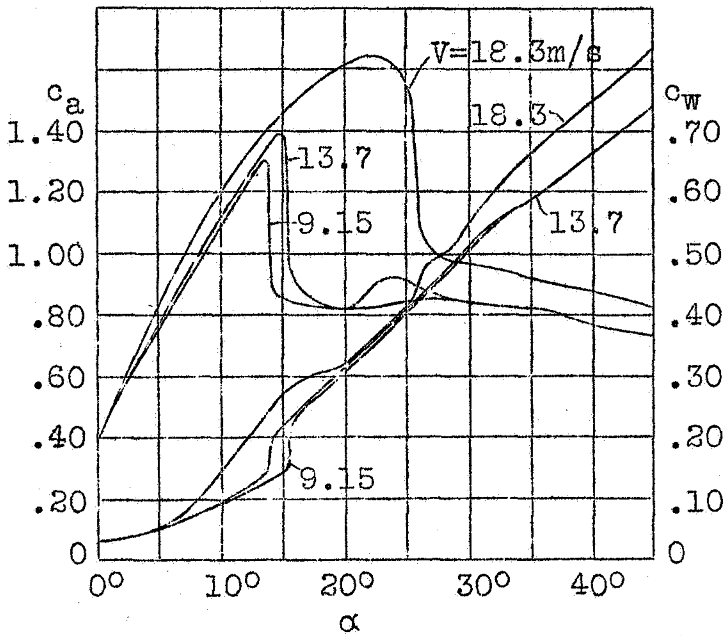

Fig.3 Airfoil No.3

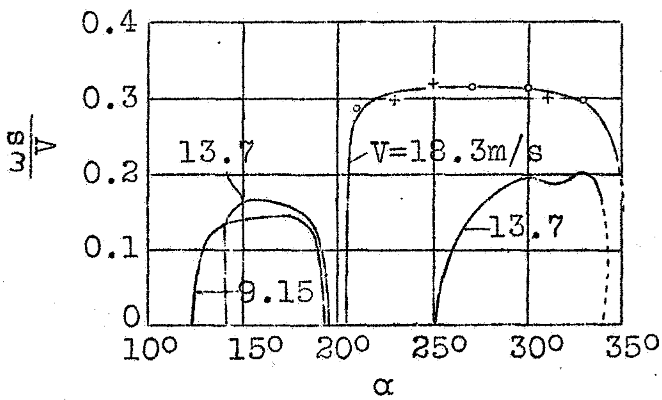

Fig.4 Airfoil No.3

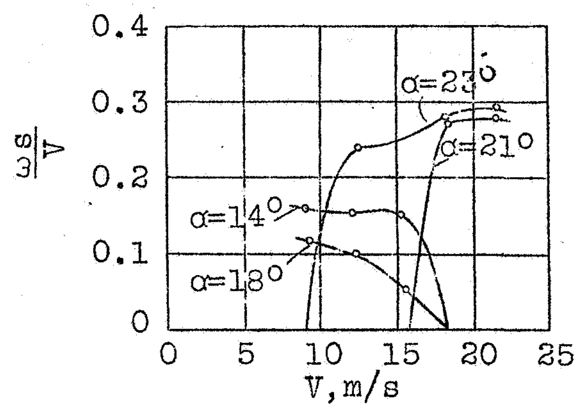

Fig.5 Airfoil No.3

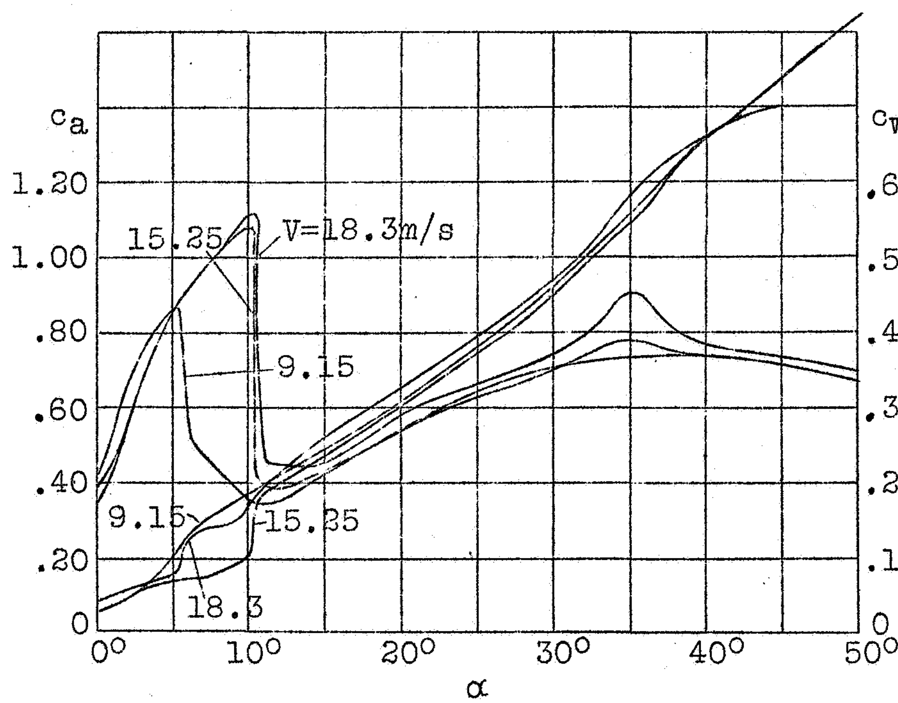

Fig.6 Airfoil No.4

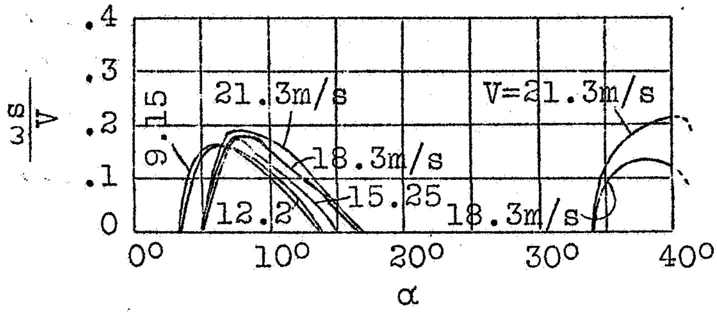

Fig.7 Airfoil No.4

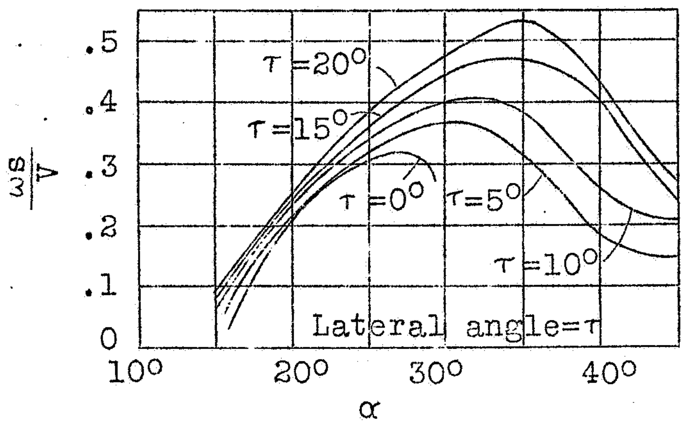

Fig.8 Airfoil No.1 V = 18.3m/s

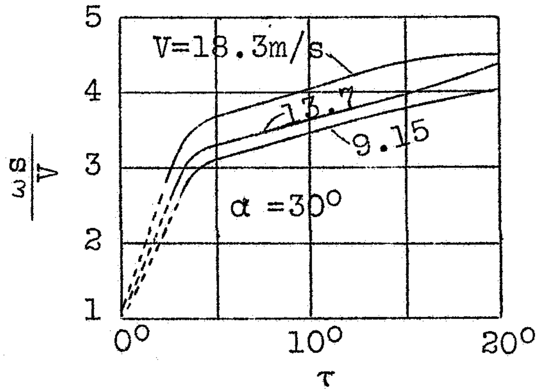

Fig.9 Airfoil No.1

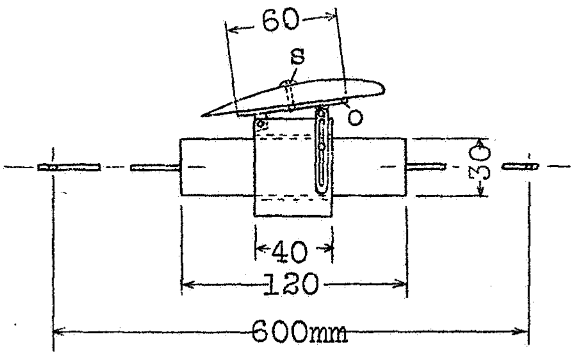

Fig.10

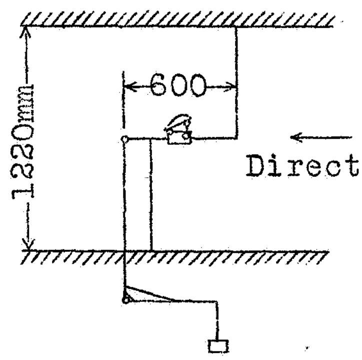

Fig.11

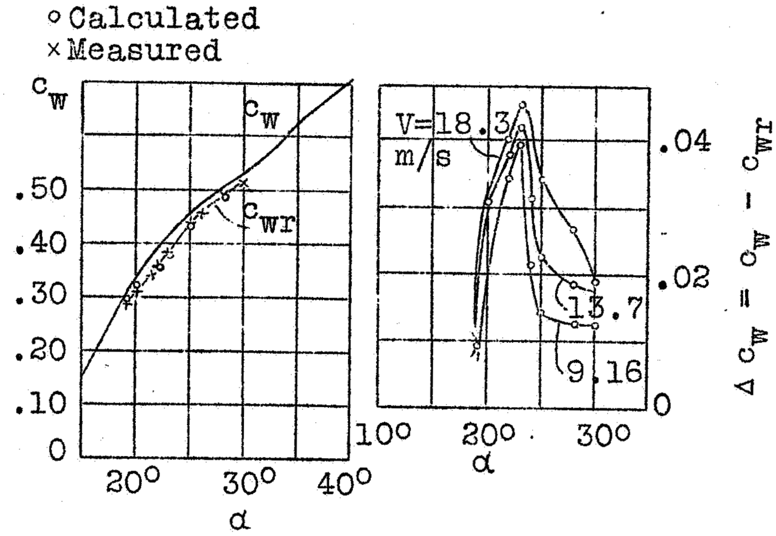

Fig.12 Airfoil No.1

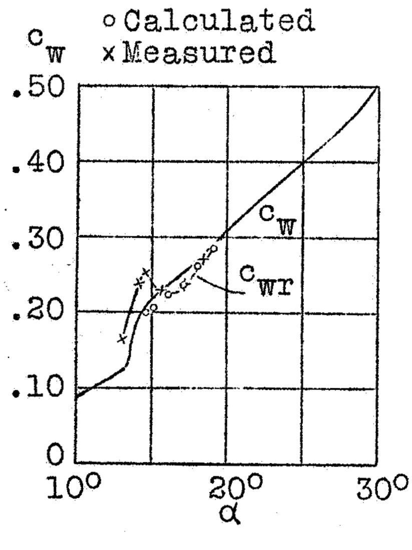

Fig.13 Airfoil No.3 V=9.15m/s
E = 5600mm m/s.

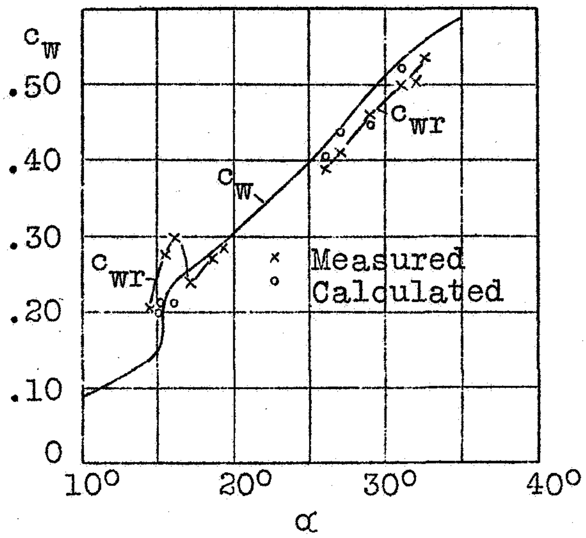

Fig.14 Airfoil No.3 V=13.7m/s
E=8400mm m/s.

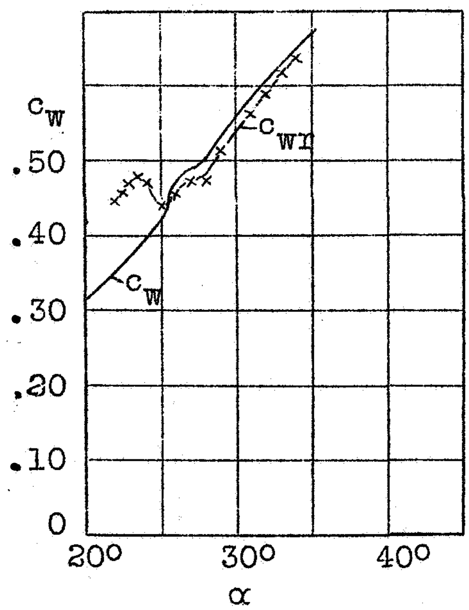

Fig.15 Airfoil No.3 V=18.3m/s
E=11120mm m/s.